CORE
Metadata, citation and similar papers at core.ac.uk
Provided by National Tsing Hua University Institutional Repository

Microwave Penetration Depth Measurement for High T_c Superconductors by Dielectric Resonators

Hang-Ting Lue, Juh-Tzeng Lue, and Tseung-Yuen Tseng, *Fellow, IEEE*

***Abstract*—The penetration depth $\lambda(T)$ dependence on temperatures for high T_c superconducting $YBa_2Cu_3O_{7-\delta}$ thin films stored in various environments was measured by a well-designed microwave dielectric resonator. A d-wave T^2 dependence was observed at low temperatures, while an exponential dependence of the penetration depth $\lambda(T)$ relevant to the s wave was detected as temperature increases due to thermal fluctuation. An abnormal upturn of the penetration depth at temperatures below 10 K attributed to the surface current carried by the defect surface-induced Andreev bound states can be apparently observed without applying heavy-ion bombardment from this relatively higher frequency measurement. Readers who endeavor to start this kind of measurement can use the well-modified dielectric cavity in conjunction with the detailed measuring procedure.**

***Index Terms*—d-wave symmetry, high T_c superconductors, microwave dielectric resonator, penetration depth, surface Andreev bound states.**

I. Introduction

THE DETERMINATION of the order symmetry of high T_c superconductors is still being hotly debated [1]–[3]. The current consensus regarding the d-wave symmetry in the hole-doped cuprates rests to a considerable extent on the success in interpretation of the anisotropy order parameter $\Delta_k(R)$ around the position R [4]. Strong scattering potentials due to nonmagnetic impurities lead to a finite energy spectral feature in the d-wave impurity band which causes a strong local suppression of the order parameter, resulting in a small change of the low-temperature properties of the penetration depth measurement [5]. Recent penetration measurements at low temperatures [6]–[8] indicate that the London penetration depth $\lambda_L(T)$ in high T_c superconductors has a mixed $s+jd$ symmetry order-parameter. An anomaly upturn of the penetration depth dependence on temperature at temperatures below $T* \approx 15$ K for heavy-ion bombarded superconducting YBCO thin films arising from the surface current induced by Andreev surface bound states was reported [9].

The deviation of the penetration depth $\lambda(T)$ from its low-temperature value $\lambda(0)$, defined as $\Delta\lambda(T) = \lambda(T) - \lambda(0)$, has an exponential $\Delta\lambda(T) \propto e^{-(\Delta/kT)}$ temperature dependence for s-wave (BCS) pairing states as calculated by Mattis–Bardeen (MB) [10], [11], and a power law T^P dependence for a d-wave [12]. An impurity or defect scattering can change the T dependence from T to T^2 [13]. In general, the results are $\Delta\lambda(T) \propto T$ for clean limit and $\Delta\lambda(T) \propto T^2$ for impurity scattering. An impurity scattered d-wave with a mixture of s-wave due to thermal fluctuation as proof of a T^2 dependence occurring at low temperatures and an exponential dependence at high temperatures was also proposed [14].

Microwave techniques allow high-precision measurements of the temperature dependence of the London penetration depth in the oxide superconductors. Many new techniques have been attempted [15]–[17] to obtain more sensitive measurement. In this work, we have probed the temperature dependence of the penetration depth by a well-designed dielectric resonator with the advantages of being easily detachable for the sample mounting and microwave coupling. The base-line shift in the Q-factor measurement is solved from the Smith chart by drawing a perfect circle with best fitting and re-plotting the S_{11} from the available data provided in the circle, resulting in a precise determination of Q. The temperature variations with stability within ±0.17 K can be easily achieved without manipulating any novel temperature controller. This measurement interposes evidence that the upturn of the $\Delta\lambda(T)$ dependence on T at very low temperatures can be observed for the defective surface of high T_c thin films without a complex modification of the sample surface. The anomaly of $\lambda(T)$ due to surface defect-induced Andreev bound states can be readily illustrated.

II. Formalism

The surface impedance Z_s of a metal film defined to be the ratio of the normal electric field over the surface magnetic field as $E_0/(\vec{n} \times \vec{H})_s$ can be derived to have the real and imaginary parts as [18]

$$R_s = \mathrm{Re}(Z_s) = \sqrt{\frac{\omega\mu_0}{2|\sigma|^2}\,(|\sigma| - \sigma_2)},$$
$$X_s = \mathrm{Im}(Z_s) = \sqrt{\frac{\omega\mu_0}{2|\sigma|^2}\,(|\sigma| + \sigma_2)} \tag{1}$$

where $\sigma(\omega) = \sigma_1(\omega) - j\sigma_2(\omega)$ is the complex conductivity of the metal. For superconductors, we have $\sigma_2(\omega) \gg \sigma_1(\omega)$ and therefore

$$R_s = \tfrac{1}{2}\,\mu_0^2\omega^2\lambda^3(T)\sigma_1(\omega, T), \quad \text{and} \quad X_s = \mu_0\omega\lambda(T). \tag{2}$$

Manuscript received December 16, 2000; revised March 22, 2002. This work was supported by the National Science Council of Taiwan, R.O.C., under Contract NSC 90-2112-M-007-001 and the Ministry of Education under Contract 90-FA04-AA.

H.-T. Lue and T.-Y. Tseng are with the Department of Electronics Engineering and Institute of Electronics, National Chiao-Tung University, Hsinchu, Taiwan, R.O.C.

J.-T. Lue is with the Department of Physics, National Tsing-Hua University, Hsinchu, Taiwan, R.O.C. (e-mail: jtlue@phys.nthu.edu.tw).

Publisher Item Identifier S 0018-9456(02)05879-5.

0018-9456/02$17.00 © 2002 IEEE

The surface resistance R_s of superconductors can be derived from the quality factor Q of the dielectric resonator where Q is defined as

$$Q = \frac{2\pi f_0 (W_E + W_M)}{\frac{1}{2} R_s \oint |H|^2 \, da} = \frac{2\pi f_0 \varepsilon_0 \varepsilon_r \oint |E|^2 \, dV}{R_s \oint |H|^2 \, da}. \quad (3)$$

In general, the Q factor can be measured from the bandwidth of the resonant frequency, which depends on the change of the penetration depth of the cavity wall. This frequency shift is conventionally derived from the Slater perturbation method that only considers the skin depth of metals. However, the power law dependence of the skin depth on frequency cannot portray the exponential dependence of London penetration dependence. We are compelled to apply the cavity perturbation theory to calculate the dependence of the frequency shift with the Q factor and the surface impedance.

III. Dielectric Resonator Design

A dielectric resonator (DR) with high dielectric constant can greatly reduce the cavity volume and yield a high quality factor for a low-loss tangent crystal. The most often used crystal is sapphire rod which has a dielectric constant of $\varepsilon_r = 12$, while an alternate $LaAlO_3$ has $\varepsilon = 25$. The detail of the DR construction is shown in Fig. 1 where a sapphire rod is installed at the center of a copper-made cylindrical cavity. The superconducting films with sizes slightly larger than the small inner diameter of the cavity are faced down on the sidewalls of the sapphire. Two copper discs engaged by springs are mounted on the films to make tight contact. A straight coaxial antenna with the polyethylene shield near the end being stripped off and forming a loop is inserted from the cavity side. The antenna soldered on a female K-connector can precisely control the insertion depth by four screws mounted on the connector that are also engaged by four springs. The coupling for the microwave power into the cavity from the antenna can be adjusted readily from the insertion depth.

The appropriate electromagnetic fields propagating inside the cavity can be solved from the Maxwell's equation with proper boundary conditions. For a cylindrical cavity with a longitudinal coordinate along the z axis and an azimuthal radius ρ, the electric and magnetic fields within the dielectric rod are [19]

$$\begin{aligned} E_{z1} &= A J_m(\xi_1 \rho) \cos(m\phi) e^{-j\beta z} \\ H_{z1} &= B J_m(\xi_1 \rho) \sin(m\phi) e^{-j\beta z} \end{aligned} \quad \text{for } 0 < \rho < a \quad (4)$$

where $\xi_1 \equiv \sqrt{(\omega/c)^2 \varepsilon_r - \beta^2}$, L is the cavity length, and $\beta = p\pi/L$ is the propagation constant. The fields within the space $a < \rho < b$ will be

$$\begin{aligned} E_{z2} &= C K_m(\xi_2 \rho) \cos(m\phi) e^{-j\beta z} + E I_m(\xi_2 \rho) \cos(m\phi) e^{-j\beta z} \\ H_{z2} &= D K_m(\xi_2 \rho) \sin(m\phi) e^{-j\beta z} + F I_m(\xi_2 \rho) \cos(m\phi) e^{-j\beta z} \end{aligned} \quad (5)$$

where $\xi_2 \equiv \sqrt{-(\omega/c)^2 + \beta^2}$. The other components along the radius ρ and azimuthal ϕ directions within the dielectric rod for $\rho < a$, and between the space $a < \rho < b$ can be derived from E_z and H_z and are illustrated in [19]. The continuities of the E and H fields at the boundary require

$$A J_m(\xi_1 a) - C K_m(\xi_2 a) - E I_m(\xi_2 a) = 0 \quad (6a)$$

$$B J_m(\xi_1 a) - D K_m(\xi_2 a) - F I_m(\xi_2 a) = 0. \quad (6b)$$

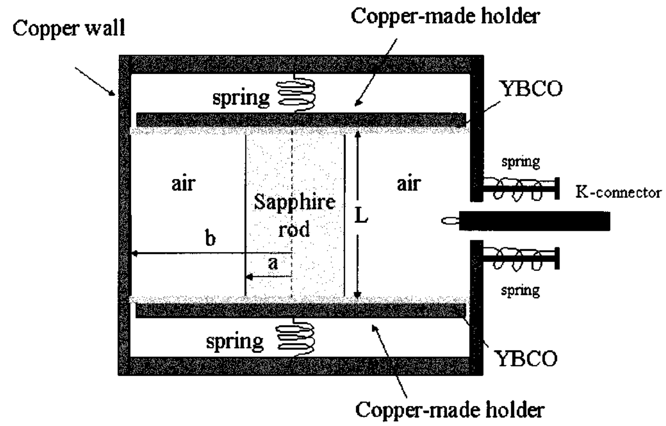

Fig. 1. Construction detail of the dielectric resonator.

In the case of nontrivial solution, the parameters A, B, C, D, E, F can be solved with the Jacobian determinant as shown in (7) at the bottom of next the page, in conjunction with the dispersion relations $\xi_1 \equiv \sqrt{(\omega/c)^2 \varepsilon_r - \beta^2}$, $\xi_2 \equiv \sqrt{-(\omega/c)^2 + \beta^2}$. If $m = 0$, the electromagnetic wave can be decoupled into either the TE or TM modes, whereas for $m > 0$, both TE and TM modes can be excited simultaneously and are referred to as the hybrid mode (HEM_{mnp}). In this work, we exploit the TE_{011} mode, which has a lower radiation loss than the TM mode outside the dielectric rod. In this mode A, C, E are zero, and (7) can be reduced to

$$\mathrm{Det} \begin{pmatrix} J_0(\xi_1 a) & -K_0(\xi_2 a) & -I_0(\xi_2 a) \\ \dfrac{J_0'(\xi_1 a)}{\xi_1} & \dfrac{K_0'(\xi^2 a)}{\xi_2} & \dfrac{I_0'(\xi_2 a)}{\xi_2} \\ 0 & K_0'(\xi_2 b) & I_0'(\xi_2 b) \end{pmatrix} = 0. \quad (8)$$

The coefficients B, D, and F are related by

$$\begin{aligned} \frac{D}{B} &= \frac{J_0(\xi_1 a) I_0'(\xi_2 b)}{K_0(\xi_2 a) I_0'(\xi_2 b) - I_0(\xi_2 a) K_0'(\xi_2 b)} \\ \frac{F}{B} &= \frac{-J_0(\xi_1 a) K_0'(\xi_2 b)}{K_0(\xi_2 a) I_0'(\xi_2 b) - I_0(\xi_2 a) K_0'(\xi_2 b)}. \end{aligned} \quad (9)$$

The energy stored inside the sapphire rod is

$$\begin{aligned} W_1 &= \frac{\varepsilon_0 \varepsilon_r}{2} \int |E_{\phi 1}|^2 \, dV \\ &= \frac{\varepsilon_0 \varepsilon_r \pi L}{2} \left(\frac{2\pi \mu_0 f}{\xi_1} \right)^2 \int_0^a |J_0'(\xi_1 \rho)|^2 \rho \, d\rho \end{aligned} \quad (10)$$

and the energy stored outside the sapphire rod is

$$\begin{aligned} W_2 &= \frac{\varepsilon_0}{2} \int |E_{\phi 2}|^2 \, dV \\ &= \frac{\varepsilon_0 \pi L}{2} \left(\frac{2\pi \mu_0 f}{\xi_2} \right)^2 \int_a^b |D K_0'(\xi_2 \rho) + F I_0'(\xi_2 \rho)|^2 \rho \, d\rho. \end{aligned} \quad (11)$$

The power loss on the sample including both the upper and lower planes is

$$
\begin{aligned}
P_s &= 2^* \tfrac{1}{2} R_s \left\{ \int_{inside} |H_{\rho 1}|^2 \, da_1 + \int_{outside} |H_{\rho 2}|^2 \, da_2 \right\} \\
&= R_s \cdot 2\pi \cdot \left\{ \left(\frac{\pi}{\xi_1 L} \right)^2 \int_0^a |J_0'(\xi_1 \rho)|^2 \rho \, d\rho + \left(\frac{\pi}{\xi_2 L} \right)^2 \int_a^b \right. \\
&\quad \cdot |DK_0'(\xi_2 \rho) + FI_0'(\xi_2 \rho)|^2 \rho \, d\rho \equiv R_s \cdot g_s
\end{aligned} \tag{12}
$$

whereas the power loss on the copper wall is

$$
\begin{aligned}
P_w &= \tfrac{1}{2} R_w \left\{ \int_{wall} |H_{z2}|^2 \, dS \right\} \\
&= \frac{R_w \pi b L}{2} \left[DK_0(\xi_2 b) + FI_0(\xi_2 b) \right] \equiv R_w \cdot g_w.
\end{aligned} \tag{13}
$$

The quality factor yields

$$
Q = \frac{2\pi f_0 (W_1 + W_2)}{g_s \cdot R_s + g_w \cdot R_w} \tag{14}
$$

where g_s and g_w are the geometric factors as specified in (12)–(14), respectively. To obtain a higher accuracy in the determination of sample resisitivity, the cavity length L should be much shorter than the radius b.

The equivalent circuit including the coupling from the antenna to the cavity can be simulated by a lossy transformer as shown in Fig. 2, from which the input impedance becomes [19]

$$
Z_{in}(\omega) = j\omega L_1 - j \frac{\omega_0^2 M^2}{2L_0 \left(\omega - \omega_0 - j \frac{\omega_0}{2Q_0} \right)} \tag{15}
$$

where L_0 and L_1 are the inductances of primary and secondary coils respectively, $\omega_0 = 1/\sqrt{L_0 C}$ and $Q_0 = \omega_0 RC = R/\omega L_0$. The cavity resistance R and inductance L_0 are composed of the surface resistance R_s and inductance attributed to the superconducting film. We can detune the resonant frequency by shifting the observing points along the transmission line by a length ℓ such that $\tan(\beta \ell) = -(\omega L_0 / Z_c)$ where $\beta = 2\pi/\lambda$. Then (15) becomes

$$
\frac{Z_{in}'(\omega)}{Z_c} = \frac{K}{1 + j2Q_0(\delta - \delta_0)} = \frac{K}{1 + j2Q_0 \delta'} \tag{16}
$$

where Z_c is the characteristic impedance and $\delta = (\omega - \omega_0)/\omega_0$, $\delta_0 = (\omega_0' - \omega_0)/\omega_0 = (K/2Q_0)(\omega L_1 / Z_c)$, $\delta' = \delta - \delta_0$, ω_0' is the new resonant frequency, and the coupling coefficient is defined by

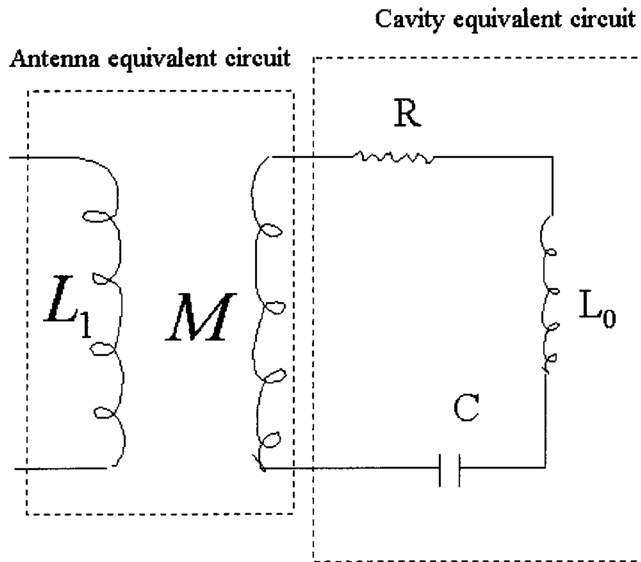

Fig. 2. Equivalent circuit of a microwave resonator. The surface resistance R_s and the effective inductance L_s of the superconducting film are included in series to the cavity resistance R and inductance L.

$$
K = \frac{(\omega M)^2}{Z_c R} \frac{1}{1 + \left(\frac{\omega L_1}{Z_c} \right)^2}. \tag{17}
$$

The condition of coupling occurs when $K < 1$, which means undercoupled, $K = 1$ which means critical coupled, and $K > 1$, which means overcoupled.

The reflection coefficient measured directly from the network analyzer will be

$$
\Gamma = \frac{Z_{in}'(\omega) - Z_c}{Z_{in}'(\omega) + Z_c} = \frac{(K - 1) - j2Q_0 \delta'}{(K + 1) + j2Q_0 \delta'}. \tag{18}
$$

The absolute value and phase angle of Γ are respectively

$$
|\Gamma| = \sqrt{\frac{(K - 1)^2 + (2Q_0 \delta')^2}{(K + 1)^2 + (2Q_0 \delta')^2}} \tag{19}
$$

and

$$
\phi = \tan^{-1} \left(\frac{\mathrm{Im}\,\Gamma}{\mathrm{Re}\,\Gamma} \right) = \tan^{-1} \left(\frac{4KQ_0 \delta'}{(2Q_0 \delta')^2 + (1 - K)^2} \right). \tag{20}
$$

$$
\begin{pmatrix}
J_m(\xi_1 a) & 0 & -K_m(\xi_2 a) & 0 & -I_m(\xi_2 a) & 0 \\
0 & J_m(\xi_1 a) & 0 & -K_m(\xi_2 a) & 0 & -I_m(\xi_2 a) \\
\frac{\beta m}{\xi_1^2 a} J_m(\xi_1 a) & \frac{\omega \mu_0}{\xi 1} J_m'(\xi_1 a) & \frac{\beta m}{\xi_2^2 a} K_m(\xi_2 a) & \frac{\omega \mu_0}{\xi_2} K_m'(\xi_2 a) & \frac{\beta m}{\xi_2^2 a} I_m(\xi_2 a) & \frac{\omega \mu_0}{\xi_2} I_m'(\xi_2 a) \\
\frac{\omega \varepsilon_r \varepsilon_0}{\xi_1} J_m'(\xi_1 a) & \frac{\beta m}{\xi_1^2 a} J_m(\xi_1 a) & \frac{\omega \varepsilon_0}{\xi_2} K_m'(\xi_2 a) & \frac{\beta m}{\xi_2^2 a} K_m(\xi_2 a) & \frac{\omega \varepsilon_0}{\xi_2} I_m'(\xi_2 a) & \frac{\beta m}{\xi_2^2 a} I_m(\xi_2 a) \\
0 & 0 & K_m(\xi_2 b) & 0 & I_m(\xi_2 b) & 0 \\
 & & \frac{\omega \varepsilon_0 m}{b} K_m(\xi_2 b) & \frac{\omega \varepsilon_0 m}{b} I_m(\xi_2 b) & \beta \xi_2 K_m'(\xi_2 b) & \beta \xi_2 I_m'(\xi_2 b)
\end{pmatrix} = 0 \tag{7}
$$

In the practical measurement, the coupling is kept undercoupled ($K < 1$) to obviate the field perturbation that implies measurement error. The Smith chart of S_{11}, in this case, shows a circle with a radius smaller than 1. Since the loaded Q-factor depends critically on the coupling constant K, the unloaded Q value can be solved by two methods as described as

i) Directly measure the reflectivity Γat the full-width of half maximum (FWHM) of the resonant curve which occurs at

$$\left|\Gamma\left(f_0 \pm \frac{\Delta f}{2}\right)\right|^2 = \frac{1 + |\Gamma_{\min}|^2}{2}. \tag{21}$$

The loaded quality factor Q_L and the unloaded quality factor Q_0 can be evaluated as $Q_L = f_0/\Delta f$, $Q_0 = (2/(1 \pm |\Gamma_{\min}|))Q_L$, and the coupling constant $K = (1 \mp \Gamma_{\min})/(1 \pm \Gamma_{\min})$, where the symbol $+$ means undercoupled, and $-$ means overcoupled conditions, respectively.

ii) Directly solve the Q_0 from curve fitting of

$$|\Gamma(f)| = C \times \sqrt{\frac{(K-1)^2 + \left(2Q_0 \frac{f - f_0'}{f_0'}\right)^2}{(K+1)^2 + \left(2Q_0' \frac{f - f_0'}{f_0'}\right)^2}} \tag{22}$$

where the constant C is derived from the deviation of the base line from 1 db, since the radiation loss is pronounced at high frequency. The constant C can be readily determined for the base line parallel to the horizontal line.

IV. Experimental Results and Discussions

A c-oriented sapphire rod of 3∼4 mm in diameter with a length of 3∼6 mm was implemented as the dielectric resonator. The dielectric constant ε_r is 11.6 along the c-axis and is 9.4 along the a–b plane. The $YBa_2Cu_3O_{7+y}$ superconducting films were deposited by laser ablation on substrates of $LaAlO_3$ and $SrTiO_3$, at film thickness of 300 nm and 400 nm, with onset critical temperatures at 82 K and 84 K, respectively. A movable insertion tube, as shown in Fig. 3, can be exploited as a temperature variation controller just by lowering down the cavity unit at different depths above the liquid helium level. The temperature can be stabilized within $\pm$0.17 K at different positions of the DR at thermal equilibrium.

In this measurement, we found that the Q_L fluctuates largely with the coupling constant K while the Q_0 derived from the method mentioned in the previous section retains a constant value within a variation of 5%. The coupling constant K as a function of temperature is plotted in Fig. 4. According to Equation (17), K is inversely proportional to R. The reason that K decreases with increasing temperature is due to the increasing input resistance (R) as temperature increases. The S_{11} reflectivity as measured from the network analyzer HP 8722D, as shown in Fig. 5, indicates that the resonant frequency and the Q factor both increase sharply as the temperature decreases. In the case when the base line of the S_{11} curve is not parallel to the horizontal 1 db line, the Smith chart will be distorted from a perfect circle. A circle is drawn by best fitting as shown in Fig. 6, and the new S_{11} is replotted from the data adopted from the Smith chart.

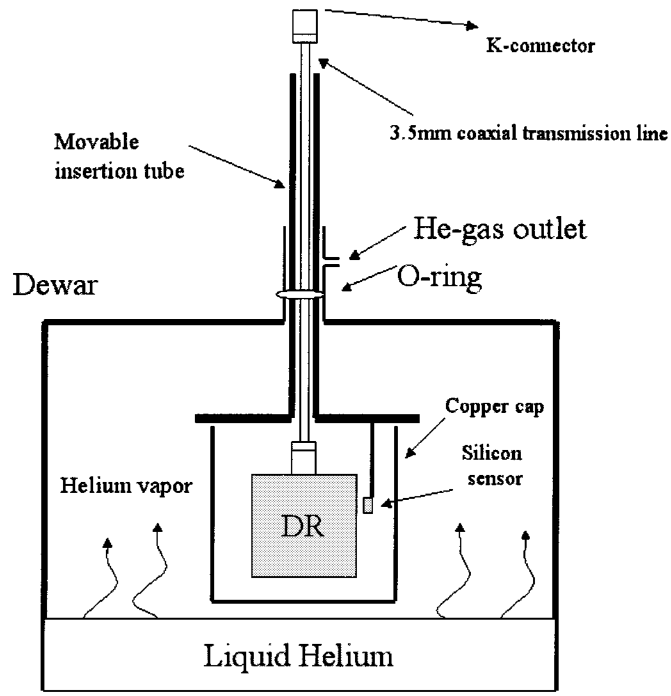

Fig. 3. Stainless steel insertion tube that can control the cavity temperature from 4.9 K to 80 K just by changing the insertion depth above the liquid helium level.

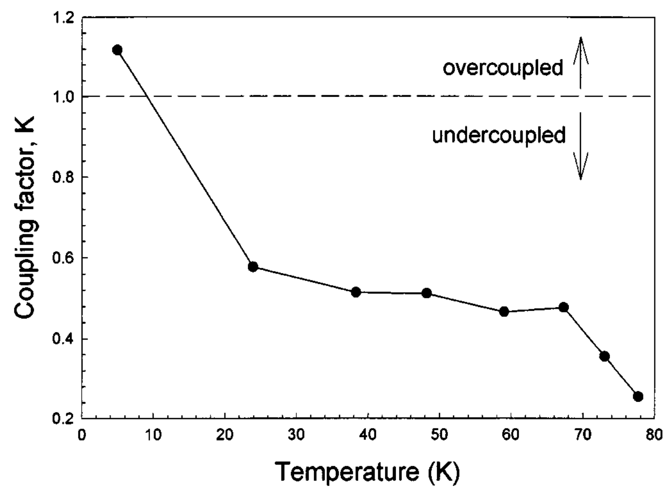

Fig. 4. Coupling coefficient, K, as a function of temperature.

The Smith chart as shown in Fig. 6 reveals that near the critical temperature T_c (at 77 K), the coupling changes from undercoupled to overcoupled near 4 K, which clearly shows the correctness of (17). This means that K increases with the decrease of resistivity R. The penetration depth $\Delta\lambda(T)$ can be deduced via (2) and (3) from the measured Q value, with the results of the temperature dependence of $\Delta\lambda(T)$ as shown in Fig. 7. The solid line is the fitting curve with the Mattis–Baddeen theory [11]

$$\frac{\lambda(T) - \lambda(4K)}{\lambda(4K)} = \sqrt{\frac{\pi\Delta}{2kT}} \exp\left(-\frac{\Delta}{kT}\right), \tag{23}$$

where $\Delta = 3.48kT_c$ is the order parameter. The d-wave predicts the power law dependence [20] $\Delta\lambda(T) \propto T^1$ or T^2 at the low temperature region, which is fitted as the dashed line. However,

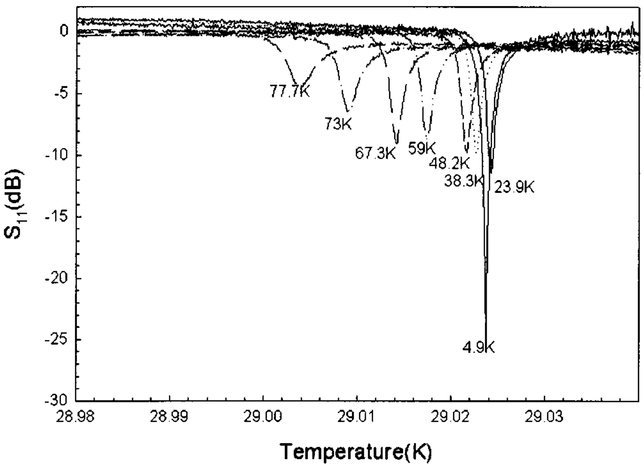

Fig. 5. S_{11} reflectivity at various temperatures for the freshly prepared YBaCO sample.

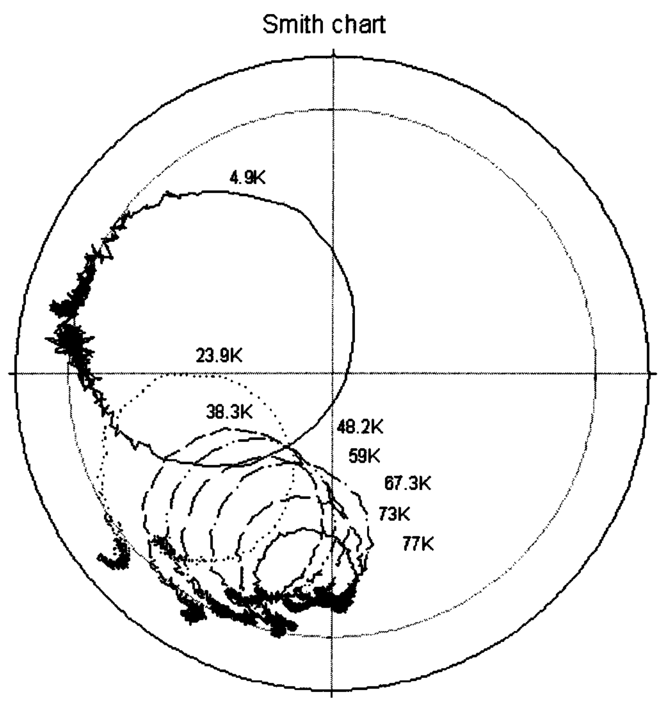

Fig. 6. Smith chart of the above sample showing the coupling changes from overcoupling to undercoupling as the cavity temperature increases from 4.9 K to 77 K.

the empirical result below 15 K reveals an abnormal upturn, advocating the existence of surface bound states even without artificial heavy-ion bombardment [9].

With the samples stored in air with high humidity for three days, the surface resistance R_s, as shown in Fig. 8(b), increases linearly with temperature T below 50 K, which is quite different from the flat results [Fig. 8(a)] of the freshly prepared samples. This fact is usually attributed to the moisture absorption and gradually desorption of oxygen atoms especially after warming from the liquid helium temperature. Since at temperatures far below $T \ll \Delta/k$ the quasinormal electrons are hardly excited for s-wave superconductors, the R_s should be kept constant. The $\Delta\lambda(T)$ for this sample as shown in Fig. 9 reveals the same evidence of the upturn below 10 K with the experimental

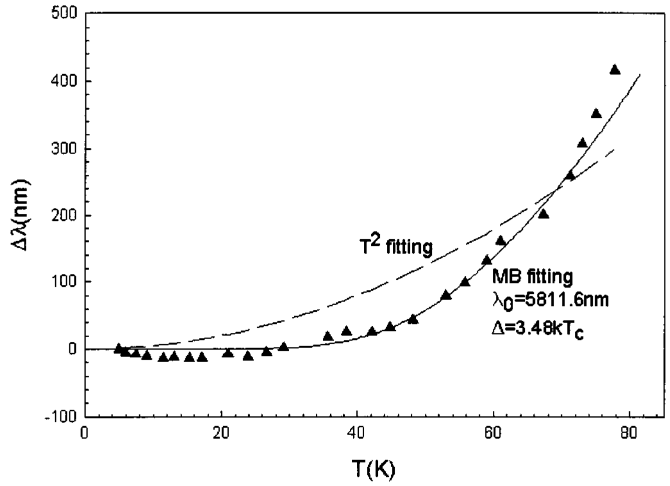

Fig. 7. Deviation of the penetration depth $\Delta\lambda(T)$ at various temperatures for the freshly prepared sample. The fitting curves of T^2 (dashed curve) and the Mattis–Bardeen theory (solid line) are also shown.

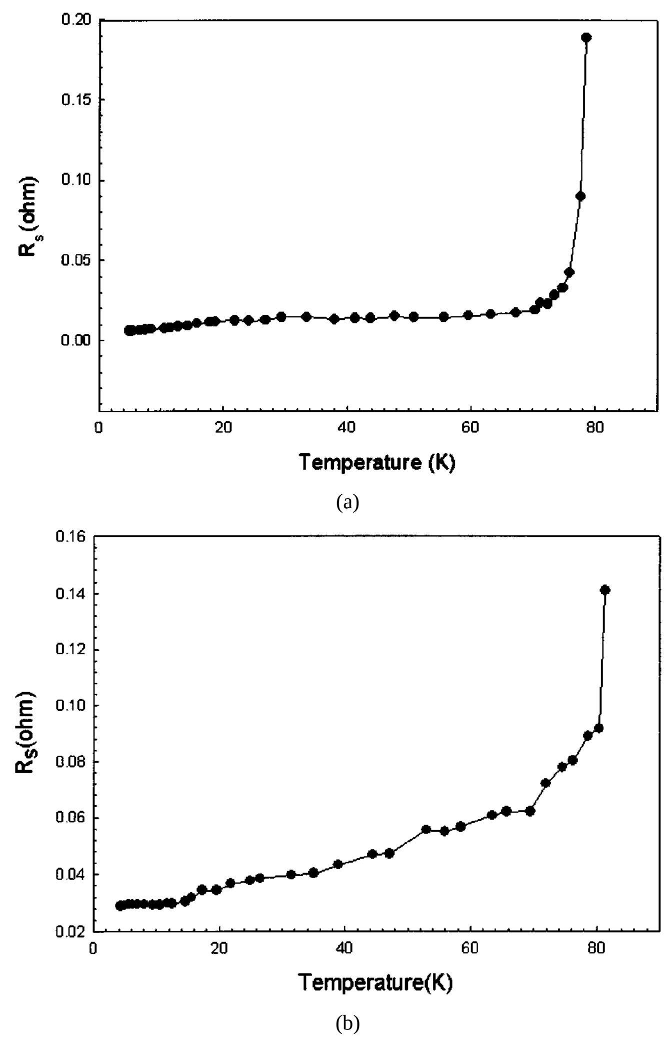

Fig. 8. Surface resistances at various temperatures for (a) the freshly prepared YBaCuO sample and (b) for the sample stored in high humidity air for three days, respectively.

data that can be fitted with the d-wave temperature dependence. This abnormal upturn at low temperatures can be prosaically ob-

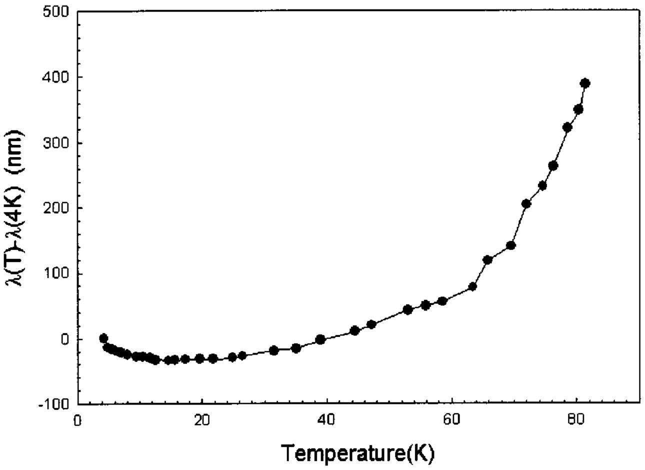

Fig. 9. Penetration depth $\Delta\lambda(T)$ for the sample stored in high humidity air for three days.

served in this work without any special surface treatment, probably arising from the higher resonant frequency (~30 GHz) that we employed in comparison with the much lower frequency (below 10 GHz) applied in other groups. Thereby, the surface effect will be prominent at higher frequency.

V. Conclusion

In this work, we have designed a microwave dielectric resonator, which is easily detachable for mounting the superconducting films and changing the coupling coefficient to measure the London penetration depth. The variation of temperatures can be readily obtained with a rather high stability just by raising and lowering a simply constructed insertion tube. The drawing of the perfect circle from the measured reflectivity data in the Smith chart and re-plotting the S_{11} adopted from the Smith circle yield results that are immune from the error attributed to the deviation of the base line from the 1 db horizontal axis due to radiation loss.

The temperature dependence of the London penetration depth measured at relatively high frequency in comparison with other groups reveals that the anomaly of the upturn below 10K attributed to surface currents carried by surface defect-induced Andreev bound states can be observed without a complex heavy-ion implantation. The power law $\Delta\lambda(T) \propto T^2$ dependence occurring at low temperatures illustrates the d-wave symmetry for the high T_c superconductors, while the exponential behavior at high temperatures alludes to the thermal fluctuation from the d-state to s-state or $d + js$ mixed state.

References

[1] R. Prozorov, R. W. Giannetta, P. Fournier, and R. L. Greene, "Evidence for nodal quasiparticles in electron-doped cuprates from penetration depth measurements," *Phys. Rev. Lett.*, vol. 85, pp. 3700–3703, 2000.

[2] I. Bonalde, B. D. Yanoff, M. B. Salamon, D. J. van Harlingen, E. M. E. Chia, Z. Q. Mao, and Y. Maeno, "Temperature dependence of the penetration depth in Sr_2RuO_4: Evidence for nodes in the gap function," *Phys. Rev. Lett.*, vol. 85, pp. 4775–4778, 2000.

[3] M. Salluzzo, F. Palomba, G. Pica, A. Andreone, I. Maggio-Aprile, O. Fisher, C. Cantoni, and D. P. Norton, "Role of Nd/Ba disorder on the penetration depth of $NdBa_2Cu_3O_{7-y}$ thin films," *Phys. Rev. Lett.*, vol. 85, pp. 1116–1119, 2000.

[4] B. J. Annett, N. Goldenfeld, and A. Leggett, *Physical Properties of High: Temperature Superconductors*, D. M. Ginsberg, Ed. Singapore: World Scientific, 1996, vol. 5, pp. 375–361.

[5] M. H. Hettler and P. J. Hirschfeld, "Scattering by impurity-induced order parameter holes in d-wave superconductors," *Phys. Rev. B*, vol. 59, pp. 9606–9610, 1999.

[6] L. J. Chen and J. T. Lue, "The transition from the d- to s-state due to thermal fluctuation for high T_c superconductors as an evidence from the microwave penetration depth measurement," *IEEE Trans. Microwave Theory Tech.*, vol. 46, pp. 1251–1256, 1998.

[7] R. Modre, I. Schurrer, and E. Schachinger, "In-plane London penetration depth superconductors with mixed-symmetry order parameters," *Phys. Rev. B*, vol. 57, pp. 5496–5504, Sept. 1998.

[8] I. Kosztin and A. J. Leggett, "Non-local effect on the magnetic penetration depth in d-wave superconductors," *Phy. Rev. Lett.*, vol. 79, pp. 135–138, 1997.

[9] H. Walter, W. Prusseit, R. Semerad, H. Kinder, W. Assmann, H. Huber, H. Burkhardt, D. Rainer, and J. A. Sauls, "Low-temperature anomaly in the penetration depth of $YBa_2Cu_3O_7$ films: Evidence for Andreev bound states at surfaces," *Phys. Rev. Lett.*, vol. 80, pp. 3598–3601, 1998.

[10] D. C. Mattis and J. Bardeen, "Theory of the anomalous skin effect in normal and superconducting metals," *Phys. Rev.*, vol. 111, pp. 412–421, 1958.

[11] J. P. Turneaure, J. Halbritter, and H. A. Schwettman, "Interpretation of the temperature dependence of the electromagnetic penetration depth in $YBa_2Cu_3O_{7-y}$,," *J. Supercond.*, vol. 4, pp. 341–355, 1991.

[12] J. F. Annett, N. Goldenfeld, and S. R. Renn, "Surface impedance of superconductors and normal conductors in metals," *Phys. Rev. B*, vol. 43, pp. 2778–2782, 1991.

[13] J. R. Cooper, "Power-law dependence of the ab-plane penetration depth in $Nd_{1.85}Ce_{0.15}CuO_{4-y}$," *Phys. Rev.*, vol. B.54, pp. R3753–R3755, 1996.

[14] L. J. Chen and J. T. Lue, "Thermal fluctuation of the order parameter symmetry in high T_c superconductors revealed from the penetration depth measurement," *Solid State Commun.*, vol. 105, pp. 155–159, 1998.

[15] C. P. Bidinosti and W. N. Hardy, "High precision ac susceptometer for measuring the temperature and magnetic field dependence of the penetration depth in superconductor single crystals," *Rev. Sci. Instrum.*, vol. 71, pp. 3816–3821, 2000.

[16] A. Gauzzi, J. Le Cochec, G. Lamura, B. J. Jonssen, V. A. Gasparov, F. R. Ladan, B. Placais, P. A. Probst, D. Pavuna, and J. Bok, "Very high resolution measurement of the penetration depth of superconductors by a novel single-soil inductance technique," *Rev. Sci. Instrum.*, vol. 71, pp. 2147–2153, 2000.

[17] V. V. Talanoz, L. V. Mercaldo, S. M. Anlaag, and H. H. Claassen, "Measurement of the penetration depth and surface resistance of superconductors and normal metals with the variable spacing parallel plate resonators," *Rev. Sci. Instrum.*, vol. 71, pp. 2136–2146, 2000.

[18] J. J. Winfield, J. P. Powell, C. E. Gough, and A. Porch, "Sensitive measurement of the surface impedance of superconducting single crystals using a sapphire dielectric resonator," *IEEE Trans. Appl. Superconduct.*, vol. 7, pp. 2009–2012, June 1997.

[19] D. M. Pozar, *Microwave Engineering*. New York: Addison-Wesley, 1990.

[20] W. Xu, Y. Ren, and C. S. Ting, "Ginzburg–Landau equations for a d-wave superconductor with nonmagnetic impurities," *Phys. Rev. B*, vol. 53, pp. 12 481–12 495, 1996.

Hang-Ting Lue was born in Hsinchu, Taiwan, R.O.C., in 1975. He received the B.S. and M.S. degrees in physics from National Tsing-Hua University (NTHU), Hsinchu, Taiwan, in 1999. He is currently pursuing the Ph.D. degree in the electrical engineering at National Chiao-Tung University (NCTU), Hsinchu.

His specialties include the quantum mechanics, electrodynamics, computer programming, semiconductor device physics and processing, microwave circuit design, and measurement techniques. His current research is focused on the application of ferroelectrics in microwave circuits, device modeling, and de-embedding techniques of RFCMOS. He is going to be a member of the Emerging Central Laboratory, Macronix International Co., Ltd., Taiwan.

Juh-Tzeng Lue was born September 22, 1943, in Taichung, Taiwan, R.O.C. He received the B.S. degree from the National Chung Kung University, Taiwan, in 1965, the M.S. degree from the National Tsing-Hua University (NTHU), Hsinchu, Taiwan, in 1969, and the Ph.D. degree from Duke University, Durham, NC, in 1974.

He is currently a Professor with the Department of Electrical Engineering and the Department of Physics, NTHU. In 1977, he was Guest Scientist Kernforschungszentrum, Karlsruhe, Germany. His areas of interest include nonlinear optics, laser systems, solid-state electronics, microwave theory and techniques, and electron spin resonance spectrometry.

Dr. Lue was a Humboldt Fellow from 1981 to 1982, he was on the Optical Society Executive Committee from 1981 to 1983, and the Solar Energy Society Executive Committee from 1980 to 1982. He received the Highest Engineering Academic prize of the R.O.C. Ministry of Education in 1982, the Distinguished Research Awards of the National Science Council, R.O.C., from 1983 to 1993, and the Distinguished Professor Awards of Lee Yuan Tzerg, from 1998 to 2003.

Tseung-Yuen Tseng (SM'94–F'02) received the Ph.D. degree in electroceramics from the School of Materials Engineering, Purdue University, West Lafayette, IN, in 1982.

Before joining National Chiao-Tung University, Hsinchu, Taiwan, R.O.C., in 1983, where he is now a Professor with the Department of Electronics Engineering and the Director of the Institute of Electronics, he was briefly associated with the University of Florida. He is a registered professional engineer in R.O.C. His professional interests are ferroelectric thin films and devices, electronic ceramics, ceramic sensors, and high temperature ceramic superconductors. He has published more than 240 technical papers.

Dr. Tseng was selected Fellow of the American Ceramic Society for "his notable contributions to the ceramic arts and sciences" in 1998 and IEEE Fellow for the contribution in ceramics and sensors in 2002. He was the recipient of the Distinguished Research Awards of the National Science Council, R.O.C., 1995 to 2000, the Distinguished Contributions Award from the Chinese Ceramic Society in 1999, and the Distinguished Electrical Engineering Professor Award from the Chinese Electrical Engineering Society in 2000.